



Share Your Innovations through JACS Directory

## Journal of Advanced Chemical Sciences

Visit Journal at <https://www.jacsdirectory.com/jacs>

## DFT Exploration on Molecular Characteristics of 6-Methyl-2-oxo-4-phenyl-1,2,3,4-tetrahydropyrimidine-5-carboxylate

Abhijit R. Bukane\*, Bapu S. Jagdale

PG Department of Chemistry, Mahatma Gandhi Vidyamandir's Arts, Science and Commerce College (Affiliated to S.P.P.U., Pune), Manmad, Nashik – 423 104, Maharashtra, India.



## ARTICLE DETAILS

## Article history:

Received 27 March 2021

Accepted 07 April 2021

Available online 09 April 2021

## Keywords:

B3LYP/6-311G(d,p)

Dihydropyrimidinone

DFT

## ABSTRACT

Present investigation deals with the synthesis and density functional theory study (DFT) of a Biginelli adduct; 6-methyl-2-oxo-4-phenyl-1,2,3,4-tetrahydropyrimidine-5-carboxylate (MOPTHPC). The synthesis of a MOPTHPC has been carried out by the reaction of benzaldehyde, ethyl acetoacetate and urea in ethanol 70-80 °C under stirring condition in presence of catalytic amount of sulfamic acid. The structure of a synthesized chalcone is affirmed on the basis of <sup>1</sup>H NMR and <sup>13</sup>C NMR. The geometry of a MOPTHPC is optimized by using the density functional theory method at the B3LYP/6-311G(d,p) basis set. The optimized geometrical parameters like bond length and bond angles have been computed. Quantum chemical parameters have been determined and examined. Molecular electrostatic surface potential (MESP) surface plot analysis has been carried out at the same level of theory. Mulliken atomic charge study is also discussed in the present study.

## 1. Introduction

The Biginelli reaction is a multi-component reaction of aldehyde, urea, and acetoacetate, involving Mannich reaction in the first step, which furnishes multifunctionalized 3,4-dihydropyrimidin-2-(1H)-ones (DHPMs) and related heterocyclic compounds. The Biginelli reaction is frequently used for the direct synthesis of 3,4-dihydropyrimidin-2-(1H)-one (DHPM) derivatives which display interesting biological activities [1,2]. Notable examples are calcium channel modulators [3], antibacterials [4], antivirals [5], antifungal [6] and other biological activities have been discovered in DHPMs [7-14]. Calculations in theoretical chemistry are based on physicochemical calculations and quantum chemistry. Different molecular properties can be predicted using density functional theory (DFT) [15-20]. UV/Vis spectra [21, 22], IR and Raman frequencies and intensities [23, 24], NMR chemical shifts [25], and spin-spin coupling constants [26] are the spectroscopic investigations that can be carried out. HOMO-LUMO energies [27-31], bond lengths and bond angles [32], and absorption energies [33-35] can all be predicted using DFT calculations. DFT method with B3LYP functional has gained a lot of interest in the last two decades. B3LYP stands for "Becke, 3-parameter, Lee-Yang-Parr". The structural and chemical properties of organic molecules have been effectively explored using the density functional theory based on theoretical quantum calculations [38-42]. As theoretical calculations are compared to experimental findings, a lot of knowledge is gained. It is now possible to arrive at a reaction mechanistic pathway using computation data. The current study looked at DFT analysis of molecular structure, bond length, bond angle, and Mulliken atomic charges. The DFT approach is also used to investigate important parameters such as total energy, HOMO-LUMO energies, and charge distribution. In last decades several green chemistry methods have been employed for the synthesis of variety of organic compounds [43-46]. In light of the above, I'd like to present a density functional theory investigation of previously synthesised 6-methyl-2-oxo-4-phenyl-1,2,3,4-tetrahydropyrimidine-5-carboxylate (MOPTHPC) compounds in this paper.

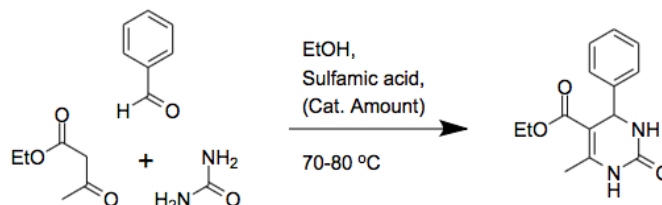
## 2. Experimental Methods

## 2.1 General Remarks

The chemicals with high purity were purchased from Virion Enterprises, India. The chemicals were used as received without any further purification. The melting point was determined in open capillary and uncorrected. <sup>1</sup>H NMR and <sup>13</sup>C NMR spectra were recorded on a sophisticated multinuclear FT-NMR spectrometer model Advance-II (Bruker) with <sup>1</sup>H frequency 500 MHz and <sup>13</sup>C frequency 125 MHz using DMSO-d<sub>6</sub> as a solvent. The reaction was monitored by thin-layer chromatography using aluminium sheets with silica gel 60 F254 (Merck).

## 2.2 Procedure for the Synthesis of Ethyl 6-Methyl-2-oxo-4-phenyl-1,2,3,4-tetrahydropyrimidine-5-carboxylate (MOPTHPC)

As shown in Scheme 1, a mixture of benzaldehyde (0.01 mol), urea (0.01 mol), and ethyl acetoacetate, (0.01 mol) were mixed in 10 mL ethanol in the conical flask and catalytic amount of sulfamic acid were added to it. The resulting mixture was stirred on a magnetic stirrer at 70-80 °C for the required time which was monitored by TLC. The crude product was transferred into a beaker containing crushed ice, stirred, filtered, dried naturally, and recrystallized from ethanol to furnish pure white solid (m.p. 196 °C -198 °C).



Scheme 1 Synthesis of MOPTHPC

## 2.3 Computational Details

All of the calculations for this work have been performed at DFT (B3LYP) methods with 6-311G(d,p) basis sets using the Gaussian 03 W program [47]. The geometry optimization of the title compound and corresponding energy were calculated with a 6-311G(d,p) basis set by assuming C<sub>1</sub> point group symmetry. Accordingly, the optimized geometrical parameters, energy, atomic charges, dipole moment, and other thermodynamic parameters were calculated theoretically.

\*Corresponding Author: [bukane.abhijit@gmail.com](mailto:bukane.abhijit@gmail.com) (Abhijit R. Bukane)

Moreover, the electronic properties, such as HOMO–LUMO energies were determined using time-dependent DFT (TD-DFT) and 6-311G(d,p) basis set, in view of the optimized structure.

### 3. Results and Discussion

#### 3.1 Spectral Analysis

The detailed spectral results are tabulated in Table 1. The  $^1\text{H}$  NMR spectrum predicts types and the total number of hydrogen atoms in the molecule. There are total of nine types of protons in the title molecule has furnished seven signals in the  $^1\text{H}$  NMR spectrum. The two NH group signals are 9.18 (s, 1H) and 7.73 (s, 1H). All other signals are correctly matched with the structure of the MOPTHPC molecule. The  $^{13}\text{C}$  NMR spectrum predicts types of carbons atoms in the molecule and therefore one can anticipate the skeleton of the molecule. There are total of twelve types of carbons that have displayed twelve signals in the  $^{13}\text{C}$  NMR spectrum affirming the structure. The two signals 165.81 and 152.60  $\delta$  are due to carbonyl carbons of ester and amide groups respectively.

**Table 1** Physicochemical and spectral data of title compound

Properties	Characteristics
Systematic Name of the Product	6-methyl-2-oxo-4-phenyl-1,2,3,4-tetrahydropyrimidine-5-carboxylate
Physicochemical data	Yield: 78%, Colour: white solid, m.p.: 196 °C-198 °C
$^1\text{H}$ NMR (400 MHz, DMSO- $d_6$ , $\delta$ )	1.09 (t, $J$ = 7.0 Hz, 3H), 2.25 (s, 3H), 3.98 (q, $J$ = 7.0 Hz, 2H), 5.14 (s, 1H), 7.25-7.33 (m, 5H), 7.73 (s, 1H), 9.18 (s, 1H)
$^{13}\text{C}$ NMR (100 MHz, DMSO- $d_6$ , $\delta$ )	14.54, 18.24, 54.43, 59.65, 99.73, 126.71, 127.73, 128.86, 145.34, 148.83, 152.60, 165.81

#### 3.2 Computational Study

##### 3.2.1 Molecular Structure, Bond Lengths and Bond Angle Analysis

The optimized molecular structure of the title molecule is depicted in Fig. 1. The optimized molecular geometry provides a good deal of information about the spatial orientation of various atoms in a molecule. From optimized molecular structures, it can be easily seen that the MOPTHPC molecule possesses C1 point group symmetry due to the overall asymmetry of the molecule. Hence, the MOPTHPC is an asymmetric top molecule. This data is a lot of helpful for the determination of various spectroscopic parameters.

The structural parameters like bond lengths and bond angles for the title molecule have been established by the DFT/B3LYP method with the 6-311G(d,p) as basis set and are presented in Table 2. The MOPTHPC molecule comprises of two six-membered rings. The DFT computation predicts the benzene ring is planar (as expected) while the other ring is non-planar. The self-consistent field (SCF) energy of the title molecule at the DFT/B3LYP method with the 6-311G(d,p) as basis set is found to be -878.57 a.u. with dipole moment 3.71 Debye. The C10-C12, C13-O20, and C11-O26 bonds are 1.3602 Å, 1.2168 Å, and 1.2161 Å long respectively. The bond angles of H30-C28-O27, C2-C1-C6 and N21-C11-N23, are 108.775°, 120.2966° and 113.3341° respectively. The bond angle and bond length data are in good agreement with the structure of the title molecule.

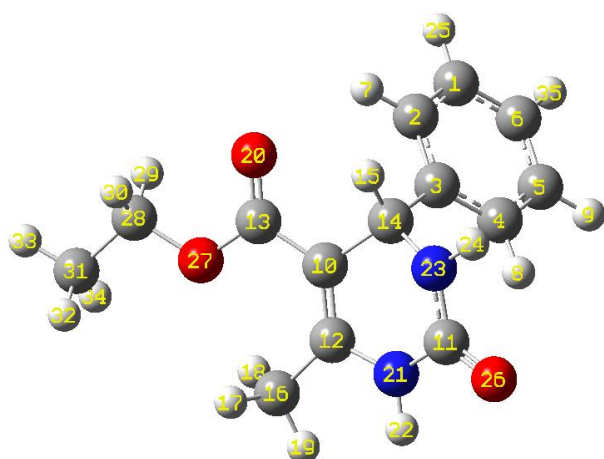


**Fig. 1** Optimized molecular structure of MOPTHPC

<https://doi.org/10.30799/jacs.236.21070105>

**Table 2** Optimized geometrical parameters of MOPTHPC by DFT/ B3LYP with 6-311G(d,p) basis set

Bond Lengths (Å)			
C1-C2	1.3923	C12-C16	1.5061
C1-C6	1.3934	C12-N21	1.3834
C1-H25	1.0845	C13-O20	1.2168
C2-C3	1.4	C13-O27	1.357
C2-H7	1.0832	C14-H15	1.0906
C3-C4	1.3984	C14-N23	1.4645
C3-C14	1.5356	C16-H17	1.0925
C4-C5	1.3938	C16-H18	1.0869
C4-H8	1.0833	C16-H19	1.0924
C5-C6	1.3923	N21-H22	1.0085
C5-H9	1.0845	C20-C23	1.5153
C6-H35	1.0843	N23-H24	1.0093
C10-C12	1.3602	O27-C28	1.4478
C10-C13	1.4662	C28-H29	1.0923
C10-C14	1.5275	C28-H30	1.0922
C10-C14	1.5278	C28-C31	1.5153
C11-N21	1.4037	C31-H32	1.0923
C11-N23	1.361	C31-H33	1.0932
C11-O26	1.2161	C31-H34	1.0924
Bond Angles (°)			
C2-C1-C6	120.2966	C3-C14-H15	107.5108
C2-C1-H25	119.6264	C3-C14-N23	113.1114
C6-C1-H25	120.0758	C10-C14-H15	107.1084
C1-C2-C3	120.6314	C10-C14-N23	108.9859
C1-C2-H7	120.2405	H15-C14-N23	107.3219
C3-C2-H7	119.1225	C12-C16-H17	110.6121
C2-C3-C4	118.6887	C12-C16-H18	111.3418
C2-C3-C14	119.3756	C12-C16-H19	110.1778
C4-C3-C14	121.9352	H17-C16-H18	107.1198
C3-C4-C5	120.6158	H17-C16-H19	108.3867
C3-C4-H8	120.4492	H18-C16-H19	109.1039
C5-C4-H8	118.9279	C11-N21-C12	124.9643
C4-C5-C6	120.308	C11-N21-H22	113.2921
C4-C5-H9	119.5902	C12-N21-H22	119.4968
C6-C5-C9	120.1005	C11-N23-C14	123.9911
C1-C6-C5	119.4564	C11-N23-H24	113.8512
C1-C6-H35	120.3039	C14-N23-H24	117.977
C5-C6-H35	120.2382	C13-O27-C28	115.6801
C12-C10-C13	126.291	O27-C28-H29	108.7957
C12-C10-C14	118.9815	O27-C28-H30	108.775
C13-C10-C14	114.6848	O27-C28-C31	107.642
N21-C11-N23	113.3341	H29-C28-H30	107.561
N21-C11-O26	121.0623	H29-C28-C31	111.9929
N23-C11-O26	125.5813	H30-C28-C31	111.9969
C10-C12-C16	127.5788	C28-C31-H32	111.0629
C10-C12-N21	118.5132	C28-C31-H33	109.6935
C16-C12-N21	113.9033	C28-C31-H34	111.1053
C10-C13-O20	123.3551	H32-C31-H33	108.2002
C10-C13-O27	114.9177	H32-C31-H34	108.5105
O20-C13-O27	121.7178	H33-C31-H34	108.1739
C3-C14-C10	112.4893	-	-

**Table 3** Mulliken atomic charges

Atom	Charge	Atom	Charge
1 C	-0.093711	19 H	0.099408
2 C	-0.062545	20 O	-0.380916
3 C	-0.045872	21 N	-0.440812
4 C	-0.080657	22 H	0.235484
5 C	-0.097981	23 N	-0.395826
6 C	-0.084594	24 H	0.235751
7 H	0.115665	25 H	0.093706
8 H	0.103071	26 O	-0.370488
9 H	0.092582	27 O	-0.368006
10 C	-0.245390	28 C	-0.020205
11 C	0.449185	29 H	0.121176
12 C	0.249113	30 H	0.121997
13 C	0.444290	31 C	-0.306426
14 C	-0.037308	32 H	0.114208
15 H	0.165526	33 H	0.112009
16 C	-0.218696	34 H	0.114550
17 H	0.141558	35 H	0.092406
18 H	0.147749	-	-

### 3.2.2 Mulliken Atomic Charges and Molecular Electrostatic Potential Surface Analysis

The Mulliken atomic charges depend on the electron density. The charge distribution on the molecules has a crucial role in the field of quantum mechanical calculations for the molecular systems. The pictorial illustration of the Mulliken atomic charges of the MOPTHPC molecule calculated by the DFT/B3LYP method with a 6-311G (d,p) basis set and tabulated in Table 3. Mulliken atomic charges reveal that all the hydrogen atoms have a net positive charge but H22 and H24 hydrogen atoms are highly electropositive with atomic charges of 0.235484 and 0.235751 respectively. This can be ascribed to attachment with a nitrogen atom in both cases. The C11 atom has the highest net positive charge 0.449185 whereas C31 atom has the highest net negative charge -0.306426 amongst all carbon atoms. Out of the three oxygen atoms, O20 is having more negative charge density of -0.380916 and out of the two nitrogen atoms; N21 is more negative with -0.440812 Mulliken atomic charges.

MESP is the three-dimensional portrayal of the charge appropriations on molecules. The MESP diagram plotted by utilizing a 6-311G(d,p) basis set is represented in Fig. 2. Over the span of on-going years, the MESP has risen as a convincing manual for investigating the molecular interactions. The phenomena like solvent effects, nucleophilic and electrophilic sites, hydrogen bonding forces, etc. could be predicted by the utilization of MESP plots. The different regions of the MESP plot are represented by different colors. The red and yellow surfaces are the regions of large electron density and therefore linked with nucleophilic sites. Similarly, the blue colors indicate low electron density and associated with electrophilic sites. On the other hand, green surfaces suggest regions of zero potential. The MESP proposes, in the MOPTHPC molecule, the benzene ring is highly reactive towards electrophiles. The two carbonyl group are showing high reactivity towards nucleophile and rest of the molecular moiety doesn't show a significant reactive site for electrophilic or nucleophilic reaction.

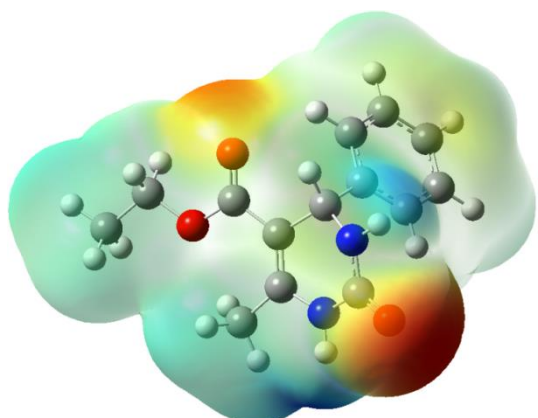


Fig. 2 MESP diagram of MOPTHPC

### 3.2.3 Frontier Molecular Orbital Analysis

The FMOs, highest occupied molecular orbital (HOMO) and lowest unoccupied molecular orbital (LUMO) are extremely crucial to anticipate the reactivity of the molecules. HOMO is the orbital which decides the nucleophilic ability whereas LUMO decides the electrophilic ability of the molecules. The energy gap between these two orbitals helps in deciding the stability. A smaller energy gap indicates high stability. Hence, one can foresee the chemical reactivity of the molecule. The expansion of the HOMO-LUMO energy gap prompts a reduction in adaptability, polarizability, and electron movement in a molecule. The HOMO energy corresponds to ionization enthalpy (I) and LUMO energy to an electron affinity (A). The pictorial outline of the FMOs has been given in Fig. 3.

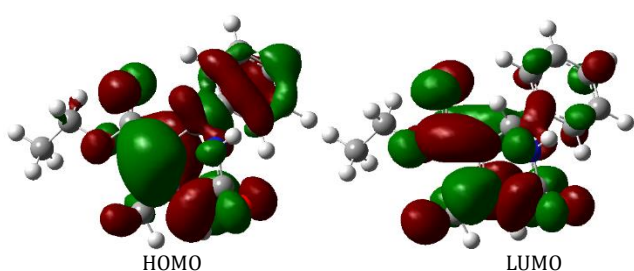


Fig. 3 HOMO-LUMO pictures of MOPTHPC

The examination of the FMOs affirms that the electron excitation corresponds to the transition from the ground state to the first excited state and is chiefly portrayed by one-electron transfer from HOMO to

LUMO. The HOMO-LUMO energy gap suggests the inevitable charge transfer phenomenon is taking place within the MOPTHPC molecule.

The various electronic parameters of the MOPTHPC molecule are tabulated in Table 4 and reactivity descriptors in Table 5. Based on HOMO and LUMO energies and by using Koopmans' theorem various global reactivity descriptors like electronegativity ( $\chi$ ) absolute hardness ( $\eta$ ) global softness ( $\sigma$ ) global electrophilicity ( $\omega$ ) chemical potential ( $\mu$ ), the maximum number of electron transferred ( $\Delta N_{max}$ ) are calculated. The electrophilicity  $\omega$  scale allowed the gathering of organic molecules as strong electrophiles with  $\omega > 1.5$  eV, moderate electrophiles with  $0.8 < \omega < 1.5$  eV and very weaker electrophiles with  $\omega < 0.8$  eV. The title molecule MOPTHPC is a good electrophile ( $\omega = 2.87$  eV). The  $\Delta N_{max}$  value of MOPTHPC molecule is 1.59 eV indicating charge transfer. The energy gap is 5.07 eV which indicates an inevitable electron movement within the title molecule.

Table 4 Electronic parameters of MOPTHPC

$E_{Total}$ (a.u.)	$E_{HOMO}$ (eV)	$E_{LUMO}$ (eV)	$\Delta E$ (eV)	I (eV)	A (eV)
-878.57	-6.35	-1.28	5.07	6.35	1.28

Note: Abbreviations: I, ionization potential; A, electron affinity; Note:  $I = -E_{HOMO}$  and  $A = -E_{LUMO}$

Table 5 Global reactivity parameters of MOPTHPC

$\chi$ (eV)	$\eta$ (eV)	$\sigma$ (eV <sup>-1</sup> )	$\omega$ (eV)	$\mu$ (eV)	$\Delta N_{max}$ (eV)	Dipole moment (Debye)
3.82	2.54	0.39	2.87	-3.82	1.59	3.71

Note:  $\chi = (I + A)/2$ ;  $\eta = (I - A)/2$ ;  $\sigma = 1/\eta$ ;  $\omega = \mu^2/2\eta$ ;  $\mu = -\chi$ ;  $\Delta N_{max} = -\mu/\eta$ . Abbreviations:  $\chi$ , electronegativity;  $\eta$ , absolute hardness;  $\sigma$ , global softness;  $\omega$ , global electrophilicity;  $\mu$ , chemical potential;  $\Delta N_{max}$ , maximum no. of electron transferred.

## 4. Conclusion

In conclusion, the MOPTHPC molecule is synthesized by a three-component Biginelli reaction. The structure of the MOPTHPC molecule is confirmed on the basis of <sup>1</sup>H NMR and <sup>13</sup>C NMR spectroscopic analysis. The geometry of the molecules was optimized by using a 6-311G(d,p) basis set and the geometrical parameters like bond lengths and bond angles have been computed at the same level of theory. The MOPTHPC molecule is an asymmetric top molecule with C<sub>1</sub> point group symmetry. The dipole moment is 3.71 Debye. The FMO study is discussed and various chemical, electronic, and quantum chemical parameters are studied to analyze the chemical reactivity of the title molecule. The HOMO-LUMO energy gap suggests that the charge transfer phenomenon is taking place within the molecule. The MESP suggest the benzene ring is highly reactive towards electrophiles. The two carbonyl group are showing high reactivity towards nucleophile.

## Acknowledgment

Author acknowledge central instrumentation facility (CIF), Savitribai Phule Pune University, Pune for NMR. Author also would like to thank Arts, Science and Commerce College, Manmad for permission and providing necessary research facilities and research assistance. Author would like to express his sincere and humble gratitude to Prof. (Dr.) A.B. Sawant for his guidance.

## References

- [1] Á. de Fátima, T.C. Braga, L.D.S. Neto, B.S. Terra, B.G. Oliveira, et al., A mini-review on Biginelli adducts with notable pharmacological properties, J. Adv. Res. 6(3) (2015) 363-373.
- [2] V.A. Adole, Synthetic approaches for the synthesis of dihydropyrimidinones/thiones (biginelli adducts): a concise review, World J. Pharm. Res. 9(6) (2020) 1067-1091.
- [3] K. Singh, D. Arora, K. Singh, S. Singh, Genesis of dihydropyrimidinone calcium channel blockers: recent progress in structure-activity relationships and other effects, Mini-Rev Med. Chem. 9(1) (2009) 95-106.
- [4] P. Attri, R. Bhatia, J. Gaur, B. Arora, A. Gupta, N. Kumar, E.H. Choi, Triethylammonium acetate ionic liquid assisted one-pot synthesis of dihydropyrimidinones and evaluation of their antioxidant and antibacterial activities, Arab. J. Chem. 10(2) (2017) 206-214.
- [5] D. Kumarasamy, B. G. Roy, J. Rocha-Pereira, J. Neyts, S. Nanjappan, et al., Synthesis and in vitro antiviral evaluation of 4-substituted 3, 4-dihydropyrimidinones, Bioorg. Med. Chem. Lett. 27(2) (2017) 139-142.

- [6] O.M. Singh, S.J. Singh, M.B. Devi, L.N. Devi, N.I. Singh, S.G. Lee, Synthesis and in vitro evaluation of the antifungal activities of dihydropyrimidinones, *Bioorg. Med. Chem. Lett.* 18(24) (2008) 6462–6467.
- [7] R. Kaur, S. Chaudhary, K. Kumar, M.K. Gupta, R.K. Rawal, Recent synthetic and medicinal perspectives of dihydropyrimidinones: A review, *Eur. J. Med. Chem.* 132 (2017) 108–134.
- [8] S. Gulati, R. Singh, R. Prakash, S. Sangwan, One-pot three component synthesis of substituted dihydropyrimidinones using fruit juices as biocatalyst and their biological studies, *PLoS One* 15(9) (2020) 0238092:1–22.
- [9] U. Divya, K. Jaspal, K. Manpreet, Antifungal activity of dihydropyrimidinones synthesized by using magnesium ferrite nanoparticles as catalyst, *Agric. Res. J.* 55(2) (2018) 313–317.
- [10] J. Lal, S.K. Gupta, D. Thavaselvam, D.D. Agarwal, Design, synthesis, synergistic antimicrobial activity and cytotoxicity of 4-aryl substituted 3, 4-dihydropyrimidinones of curcumin, *Bioorg. Med. Chem. Lett.* 22(8) (2012) 2872–2876.
- [11] K.P. Beena, R. Suresh, A. Rajasekaran, P.K. Manna, Dihydropyrimidinones-a versatile scaffold with diverse biological activity, *J. Pharm. Sci. Res.* 8(8) (2016) 741–746.
- [12] G.O. de Azambuja, L. Svetaz, I.L. Gonçalves, P.F. Corbellini, G.L. von Poser, et al., In vitro antifungal activity of dihydropyrimidinones/thiones against *Candida albicans* and *Cryptococcus neoformans*, *Curr. Bioact. Compd.* 15(6) (2019) 648–655.
- [13] J.P. Wan, Y. Pan, Recent advance in the pharmacology of dihydropyrimidinone, *Mini-Rev Med. Chem.* 12(4) (2012) 337–349.
- [14] S. Chitra Antibacterial and antifungal studies 5-ethoxycarbonyl-4-Aryl-6-methyl-3, 4-dihydropyrimidinones, *Int. Res. J. Pharmaceut. Appl. Sci.* 2(6) (2012) 71–73.
- [15] R. Thomas, M. Hossain, Y.S. Mary, K.S. Resmi, S. Armarković, et al., Spectroscopic analysis and molecular docking of imidazole derivatives and investigation of its reactive properties by DFT and molecular dynamics simulations, *J. Mol. Struct.* 1158 (2018) 156–175.
- [16] V.A. Adole, R.H. Waghchaure, S.S. Pathade, M.R. Patil, T.B. Pawar, B.S. Jagdale, Solvent-free grindstone synthesis of four new (E)-7-(arylidene)-indanones and their structural, spectroscopic and quantum chemical study: a comprehensive theoretical and experimental exploration, *Mol. Simul.* 46 (2020) 1045–1054.
- [17] M. Bouklah, H. Harek, R. Touzani, B. Hammouti, Y. Harek, DFT and quantum chemical investigation of molecular properties of substituted pyrrolidinones, *Arab. J. Chem.* 5(2) (2012) 163–166.
- [18] V.A. Adole, T.B. Pawar, B.S. Jagdale, DFT computational insights into structural, electronic and spectroscopic parameters of 2-(2-Hydrazineyl) thiazole derivatives: a concise theoretical and experimental approach, *J. Sulfur Chem.* 42(2) (2021) 131–148.
- [19] H.A. Ahmed, M. Hagar, O.A. Alhaddad, New chair shaped supramolecular complexes-based aryl nicotinate derivative; mesomorphic properties and DFT molecular geometry, *RSC Adv.* 9(29) (2019) 16366–16374.
- [20] J. Frau, D. Glossman-Mitnik, A conceptual DFT study of the molecular properties of glycating carbonyl compounds, *Chem. Cent. J.* 11(1) (2017) 1–8.
- [21] S.L. Dhonnar, V.A. Adole, N.V. Sadgir, B.S. Jagdale, Structural, spectroscopic (UV-Vis and IR), electronic and chemical reactivity studies of (3, 5-diphenyl-4, 5-dihydro-1H-pyrazol-1-yl)(phenyl) methanone, *Phys. Chem. Res.* 9(2) (2021) 193–209.
- [22] A. Ayeshamariam, S. Ramalingam, M. Bououdina, M. Jayachandran, Preparation and characterizations of SnO<sub>2</sub> nanopowder and spectroscopic (FT-IR, FT-Raman, UV-Visible and NMR) analysis using HF and DFT calculations, *Spectrochim. Acta A Mol. Biomol. Spectrosc.* 118 (2014) 1135–1143.
- [23] M. Raja, R.R. Muhamed, S. Muthu, M. Suresh, Synthesis, spectroscopic (FT-IR, FT-Raman, NMR, UV-Visible), first order hyperpolarizability, NBO and molecular docking study of (E)-1-(4-bromobenzylidene) semicarbazide, *J. Mol. Struct.* 1128 (2017) 481–492.
- [24] P. Manjusha, S. Muthu, B.R. Raajaraman, Density functional studies and spectroscopic analysis (FT-IR, FT-Raman, UV-visible, and NMR) with molecular docking approach on an antifibrotic drug Pirfenidone, *J. Mol. Struct.* 1203 (2020) 127394.
- [25] M. Bühl, M. Kaupp, O.L. Malkina, V.G. Malkin, The DFT route to NMR chemical shifts, *J. Comput. Chem.* 20(1) (1999) 91–105.
- [26] V.G. Malkin, O.L. Malkina, D.R. Salahub, Calculation of spin—spin coupling constants using density functional theory, *Chem. Phys. Lett.* 221 (1994) 91–99.
- [27] E. Barim, F. Akman, Synthesis, characterization and spectroscopic investigation of N-(2-acetylbenzofuran-3-yl) acrylamide monomer: Molecular structure, HOMO–LUMO study, TD-DFT and MEP analysis, *J. Mol. Struct.* 1195 (2019) 506–513.
- [28] S.S. Pathade, V.A. Adole, B.S. Jagdale, T.B. Pawar, Molecular structure, electronic, chemical and spectroscopic (UV-visible and IR) studies of 5-(4-chlorophenyl)-3-(3, 4-dimethoxyphenyl)-1-phenyl-4, 5-dihydro-1H-pyrazole: combined DFT and experimental exploration, *Mat. Sci. Res. India* 17(specialissue2020) (2020) 27–40.
- [29] P. Vennila, M. Govindaraju, G. Venkatesh, C. Kamal, Molecular structure, vibrational spectral assignments (FT-IR and FT-Raman), NMR, NBO, HOMO–LUMO and NLO properties of O-methoxybenzaldehyde based on DFT calculations, *J. Mol. Struct.* 1111 (2016) 151–156.
- [30] R.A. Shinde, V.A. Adole, B.S. Jagdale, T.B. Pawar, B.S. Desale, R.S. Shinde, Efficient Synthesis, spectroscopic and quantum chemical study of 2, 3-dihydrobenzofuran labelled two novel arylidene indanones: A comparative theoretical exploration, *Mat. Sci. Res. India* 17(2) (2020) 146–161.
- [31] M.K. Priya, B.K. Revathi, V. Renuka, S. Sathya, P.S. Asirvatham, Molecular structure, spectroscopic (FT-IR, FT-Raman, <sup>13</sup>C and <sup>1</sup>H NMR) analysis, HOMO–LUMO energies, Mulliken, MEP and thermal properties of new chalcone derivative by DFT calculation, *Mater. Today* 8 (2019) 37–46.
- [32] V.A. Adole, B.S. Jagdale, T.B. Pawar, B.S. Desale, Molecular structure, frontier molecular orbitals, MESP and UV-visible spectroscopy studies of Ethyl 4-(3, 4-dimethoxyphenyl)-6-methyl-2-oxo-1,2,3,4-tetrahydropyrimidine-5-carboxylate: A theoretical and experimental appraisal, *Mat. Sci. Res. India* 17(specialissue2020) (2020) 13–36.
- [33] M.A. Iramain, A.E. Ledesma, E. Imbarack, P.L. Bongiorno, S.A. Brandán, Spectroscopic studies on the potassium 1-fluorobenzoyltrifluoroborate salt by using the FT-IR, Raman and UV-Visible spectra and DFT calculations, *J. Mol. Struct.* 1204 (2020) 127534.
- [34] V. Arjunan, T. Rani, C.V. Mythili, S. Mohan, Synthesis, FTIR, FT-Raman, UV-visible, ab initio and DFT studies on benzohydrazide, *Spectrochim. Acta A Mol. Biomol. Spectrosc.* 79(3) (2011) 486–496.
- [35] V.A. Adole, R.H. Waghchaure, B.S. Jagdale, T.B. Pawar, Investigation of structural and spectroscopic parameters of ethyl 4-(4-isopropylphenyl)-6-methyl-2-oxo-1,2,3,4-tetrahydropyrimidine-5-carboxylate: a DFT Study, *Chem. Bio. Interf.* 10(1) (2020) 22–30.
- [36] T.B. Pawar, B.S. Jagdale, A.B. Sawant, V.A. Adole, DFT studies of 2-[(2-substitutedphenyl) carbamoyl] benzoic acids, *J. Chem. Biol. Phys. Sci.* 7 (2017) 167–175.
- [37] R.A. Shinde, V.A. Adole, B.S. Jagdale, T.B. Pawar, Experimental and theoretical studies on the molecular structure, FT-IR, NMR, HOMO, LUMO, MESP, and reactivity descriptors of (E)-1-(2,3-dihydrobenzo [b][1,4] dioxin-6-yl)-3-(3, 4, 5-trimethoxyphenyl) prop-2-en-1-one, *Mat. Sci. Res. India*, 17(specialissue2020) (2020) 54–72.
- [38] V.A. Adole, P.B. Koli, R.A. Shinde, R.S. Shinde, Computational insights on molecular structure, electronic properties, and chemical reactivity of (E)-3-(4-chlorophenyl)-1-(2-hydroxyphenyl) prop-2-en-1-one, *Mat. Sci. Res. India*, 17(specialissue2020) (2020) 41–53.
- [39] V.A. Adole, R.H. Waghchaure, B.S. Jagdale, T.B. Pawar, S.S. Pathade, Molecular structure, frontier molecular orbital and spectroscopic examination on dihydropyrimidinones: a comparative computational approach, *J. Adv. Sci. Res.* 11(2) (2020) 64–70.
- [40] R.H. Waghchaure, T.B. Pawar, Synthesis, characterization, molecular structure, and HOMO–LUMO study of 2-phenylquinoxaline: a DFT exploration, *World J. Pharm. Res.* 9(6) (2020) 1867–1881.
- [41] V.A. Adole, V.R. Bagul, S.A. Ahire, R.K. Pawar, G.B. Yelame, A.R. Bukane, Computational chemistry: molecular structure, spectroscopic (UV-visible and IR), electronic, chemical and thermochemical analysis of 3'-phenyl-1,2-dihydrospiro[indeno[5,4-b], J. Adv. Sci. Res. 12(1) (2021) 276–286.
- [42] V.A. Adole, B.S. Jagdale, T.B. Pawar, A.B. Sawant, Experimental and theoretical exploration on single crystal, structural, and quantum chemical parameters of (E)-7-(arylidene)-1,2,6,7-tetrahydro-8H-indeno [5,4-b] furan-8-one derivatives: A comparative study, *J. Chin. Chem. Soc.* 67(10) (2020) 1763–1777.
- [43] V.A. Adole, T.B. Pawar, P.B. Koli, B.S. Jagdale, Exploration of catalytic performance of nano-La<sub>2</sub>O<sub>3</sub> as an efficient catalyst for dihydropyrimidinone/thione synthesis and gas sensing, *J. Nanostruct. Chem.* 9(1) (2019) 61–76.
- [44] V.A. Adole, R.A. More, B.S. Jagdale, T.B. Pawar, S.S. Chobe, Efficient synthesis, antibacterial, antifungal, antioxidant and cytotoxicity study of 2-(2-hydrazineyl)thiazole derivatives, *Chem. Select* 5(9) (2020) 2778–2786.
- [45] V.A. Adole, B.S. Jagdale, T.B. Pawar, A.A. Sagane, Ultrasound promoted stereoselective synthesis of 2, 3-dihydrobenzofuran appended chalcones at ambient temperature, *S. Afr. J. Chem.* 73 (2020) 35–43.
- [46] S.S. Chobe, V.A. Adole, K.P. Deshmukh, T.B. Pawar, B.S. Jagdale, Poly (ethylene glycol)(PEG-400): A green approach towards synthesis of novel pyrazolo [3,4-d] pyrimidin-6-amines derivatives and their antimicrobial screening, *Arch. Appl. Sci. Res.* 6(2) (2014) 61–66.
- [47] M.J. Frisch, G.W. Trucks, H.B. Schlegel, G.E. Scuseria, M.A. Robb, Gaussian 03, Revision C.02, Gaussian, Inc., Wallingford CT, 2004.